PHYSICAL REVIEW B **95**, 041108(R) (2017)

Kondo screening of the spin and orbital magnetic moments of Fe impurities in Cu

L. Joly,[1] J.-P. Kappler,[2] P. Ohresser,[2] Ph. Sainctavit,[3] Y. Henry,[1] F. Gautier,[1] G. Schmerber,[1] D. J. Kim,[1,*] C. Goyhenex,[1] H. Bulou,[1] O. Bengone,[1] J. Kavich,[4] P. Gambardella,[5] and F. Scheurer[1,†]

[1]*Université de Strasbourg, CNRS, IPCMS, UMR 7504, F-67000 Strasbourg, France*

[2]*Synchrotron-SOLEIL, L'Orme des Merisiers Saint-Aubin, BP 48, F-91192 Gif-sur-Yvette Cedex, France*

[3]*Institut de Minéralogie, de Physique des Matériaux et de Cosmochimie, UMR 7590 CNRS, UPMC, IRD et MNHN, F-75005 Paris, France*

[4]*Catalan Institute of Nanoscience and Nanotechnology (ICN2), UAB Campus, E-08193 Bellaterra, Spain*

[5]*Department of Materials, ETH Zürich, Hönggerbergring 64, CH-8093 Zurich, Switzerland*

(Received 4 June 2016; revised manuscript received 8 December 2016; published 20 January 2017)

We use x-ray magnetic circular dichroism to evidence the effect of correlations on the local impurity magnetic moment in an archetypal Kondo system, namely, a dilute Cu:Fe alloy. Applying the sum rules on the Fe $L_{2,3}$ absorption edges, the evolution of the spin and orbital moments across the Kondo temperature are determined separately. The spin moment presents a crossover from a nearly temperature-independent regime below the Kondo temperature to a paramagneticlike regime above. Conversely, the weak orbital moment shows a temperature-independent behavior in the whole temperature range, suggesting different Kondo screening temperature scales for the spin and orbital moments.

DOI: 10.1103/PhysRevB.95.041108

The Kondo effect [1] is a consequence of many-body interactions that originates from the hybridization of localized strongly correlated electrons with a continuum of free-electron-like metal states. According to the Anderson impurity model [2] and the related *s-d* Kondo model [3,4], the spin of an $S = \frac{1}{2}$ impurity is effectively screened by the continuum states of the metal host upon the formation of a coherent many-body singlet state, which occurs below the Kondo temperature T_K [3,5]. At T_K, the system exhibits a crossover [6] from a low-temperature local Fermi liquid state [3,5] to a high-temperature regime characterized by a free-spin behavior corrected by logarithmic temperature terms. It was noted early that a realistic description of the Kondo effect should take into account the orbital degrees of freedom in addition to the localized exchange interaction and spin multiplicity of the impurities [7,8].

Despite recent theoretical progress using *ab initio* methods, keeping track of all the relevant parameters for transition metal impurities in nonmagnetic hosts, such as crystal field or spin-orbit coupling, remains extremely difficult [9–13]. For example, theoretical studies of Fe impurities in Au [9,10] propose different low-energy scenarios, namely, the *n*-channel model [14] and the orbital-dependent Kondo effect [15], to interpret magnetotransport and decoherence experiments. On another hand, studies combining density functional theory (DFT) and quantum Monte Carlo [10,13], as well as the noncrossing approximation [12], reveal the importance of multiorbital effects and the difficulty to determine a reliable T_K. For the Cu:Fe dilute alloy, an archetypal Kondo system [3,16–18], the *n*-channel model with $n = 4$ and $S = 2$, has been shown to fit the magnetization data deduced from Mössbauer spectroscopy and specific heat [19]. These results suggest, without further theoretical justification, that the ground state of the Fe impurities is both a spin and an orbital singlet.

An intrinsic difficulty for experiments is to probe the spin and orbital magnetic moments in a separate way. Classical magnetometry techniques measure the macroscopic susceptibility and do not provide information at the level of the impurity itself. Local techniques such as Mössbauer spectroscopy and nuclear magnetic resonance (NMR) probe the microscopic susceptibility, but rely on the assumptions that spin and orbital components are proportional to the hyperfine field, and that the orbital component is constant with temperature [17,18,20]. Scanning tunneling microscopy has recently provided useful information about the spatial and structural dependence of the Kondo resonance [21–23], including Fe on Cu [24], but the details of the magnetic configuration remain unaccessible. X-ray magnetic circular dichroism (XMCD), on the other hand, has the unique capability to separately probe m_s and m_l in a direct and quantitative way [25,26], besides being sensitive to dilute amounts of transition metal impurities [27–30]. So far, it has, however, not been used to investigate the temperature dependence of the local magnetic moment in a Kondo system.

Here, we investigate the crossover from the paramagnetic limit to the Kondo-screened state of Fe impurities in Cu using XMCD. We provide a separate measurement of the spin and orbital magnetic moments as a function of temperature in a dilute Kondo system. Two main consequences of Kondo correlations are evidenced: (i) a strong reduction of the impurity spin saturation moment compared to a paramagnetic impurity, and (ii) a temperature-independent behavior for m_s below the Kondo temperature. Furthermore, m_l is constant over the considered temperature range, suggesting that m_s and m_l are screened differently.

We chose the dilute Cu:Fe alloy system, because of its historical relevance [3,16–19,24,31] but mostly because its Kondo temperature ($T_K \approx 20$–30 K) provides a relatively broad temperature range below and above T_K to probe the Fe magnetic moment. We performed XMCD measurements between 2 and 150 K, limited by the decrease of the

*Present address: Department of Physics, University of Warwick, Coventry CV4 7AL, UK.

†fabrice.scheurer@ipcms.unistra.fr

magnetic signal with temperature in the paramagnetic phase. The fabrication of dilute alloys requires addressing two difficulties. The first is the formation of magnetically coupled Fe pairs, which occurs when the Fe concentration exceeds about 1000 ppm. Since the Kondo temperature of Fe pairs (T_K^{pair}) is much lower than T_K for isolated impurities, the paramagnetic pair signal would dominate the impurity moment at temperatures between T_K^{pair} and T_K [32,33]. The second is related to sample oxidation which must be specifically taken into account for the interpretation of the intrinsically surface-sensitive XMCD measurements. Because Cu is not a good barrier against oxygen penetration, Fe oxidation takes place near the sample surface. As shown below, however, the x-ray absorption signal of Fe oxide can be identified and subtracted from the absorption spectra of Fe. Two types of polycrystalline dilute Cu:Fe alloys were prepared: bulk alloys, obtained by a melting preparation technique [32], and thin films obtained by magnetron sputtering in ultrahigh vacuum conditions (base pressure in the low 10^{-9} mbar range). The latter method was used successfully in earlier work on the Kondo effect [34]. Films of 200–350 nm were deposited on transparent SiC membranes (200 μm thick). They were grown at room temperature by codeposition from a pure Cu target and a mixed Cu:Fe one containing 1 at. % Fe. The evaporation rates ($\approx$1 nm/s) were adjusted to obtain the desired composition. After fabrication, the samples were kept at $\approx$100 K to avoid atomic diffusion which may lead to clustering of the Fe impurities (i.e., yielding a paramagnetic pair magnetization) [32]. In order to verify the presence of a Kondo effect, the electrical resistivity of the samples was measured as a function of temperature using conventional four-point resistance measurements.

The XMCD experiments were performed at the SIM beamline of the Swiss Light Source on the French cryomagnet end station. The x-ray absorption spectra (XAS) were recorded at the $L_{2,3}$ edges of Fe in a $\pm$6.5 T magnetic field in the 2–150 K temperature range. The field was parallel to the incident photon beam, and normal to the sample surface. XMCD spectra were obtained by switching both the x-ray helicity and the direction of the magnetic field in order to remove any possible spurious asymmetries and yield reliable dichroic signals. The spectra were recorded using the "on-the-fly mode" [35], the light helicity being switched after a full absorption spectrum. The magnetic field was inverted after acquisition of a set of several spectra.

We checked that the smallest concentration that can be measured within a 1-week beam time was in the order of 500 ppm. At each temperature, about 80 energy scans, representing 6 h of acquisition time, were averaged to obtain the XMCD signal. The bulk samples were analyzed by total electron yield (TEY) and the thin film samples by TEY and transmission. Because of the very small magnetic signal per impurity and low Fe concentration, XMCD was only measured with the largest available field. In order to provide a comparison of the experimental results with the magnetic moment of Fe expected in the absence of Kondo correlation effects, we performed an extensive series of DFT and Ligand field multiplet calculations (LFMs). While DFT provides an accurate description of the bare Fe spin moment at 0 K, LFM allows comparing the spin and orbital moments of Fe ions in a 3*d* configuration as a function of temperature and magnetic field, for different crystal field symmetries and Slater correlation parameters.

Two samples were investigated: a 2500 ppm bulk sample, and a 500 ppm thin film sample. The first yields a larger Fe signal, but with an important pair interaction, whereas the second provides a negligible pair interaction. The Fe concentrations were estimated by measuring the edge jump intensity at the Fe L_3 edge and agree within $\approx$10% with the nominal concentrations. The measured Kondo minima of the resistivity are respectively 21 K (500 ppm) and 40 K (2500 ppm), in excellent agreement with earlier measurements [31]. In the following we will focus on the 500 ppm thin film sample. The results for the 2500 ppm are discussed in the Supplemental Material [36].

The x-ray absorption spectra of the Fe $L_{2,3}$ edges show a strong oxide contribution. One must therefore first isolate the Fe impurity contribution by subtracting the oxide part in the spectra (see the Supplemental Material [36], Fig. S1). Figure 1 shows oxide-corrected XAS and XMCD spectra at 100 and 2 K. No obvious spectral changes are observed in the XAS when going from the paramagnetic to the Kondo regime. Since the system is metallic, possible modifications due to the Kondo correlations are too faint to be observable. The main qualitative observation is a reduced XMCD intensity at 100 K as compared to the XMCD at 2 K, indicating a smaller spin moment at high temperature.

The projection of the spin (m_s) and orbital (m_l) magnetic moments along the photon beam (parallel to the magnetic field) was determined by applying the XMCD sum rules [25,26,36]. Since the samples are polycrystalline and present a local cubic environment, the magnetic dipolar term (T_z) to the spin sum rule can be safely neglected, as it is usual for bulk metal compounds [37]. Figure 2 shows the m_l/m_s ratio as a function of temperature, obtained after subtracting the oxide contribution from the Fe XMCD spectra. This ratio depends only on the relative intensity of the L_3 and L_2 components of the dichroic signal, and can thus be obtained self-consistently

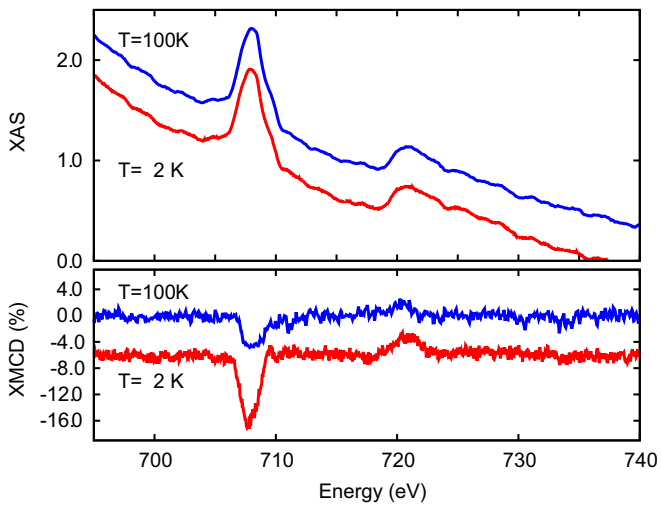

FIG. 1. Oxide-subtracted XAS (top) and XMCD (bottom) transmission spectra of a 500 ppm Cu:Fe sample deposited on a SiC membrane for 100 and 2 K, with an applied magnetic field of $\pm$6.5 T. The spectra have been offset for clarity.

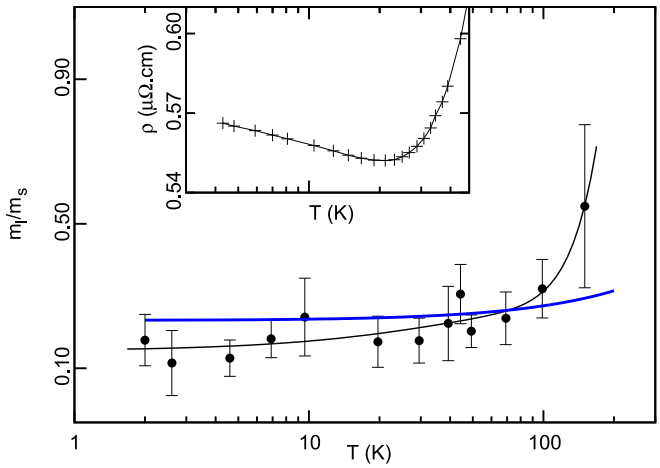

FIG. 2. Orbital to spin moment ratio m_l/m_s as a function of temperature for the 500 ppm sample in a 6.5 T field, as determined by sum rules. The thin (black) line is a guide to the eye. The thick (blue) solid line is a LFM calculation for an Fe ion in a $3d^7$ configuration in cuboctahedral symmetry with $10Dq = 0.25$ eV and a reduction of the atomic Slater integral parameters of $\kappa = 0.8$. Inset: Low-temperature resistivity as a function of T for the 500 ppm sample on a semilogarithmic scale. Note the characteristic $\ln(T)$ Kondo behavior of the resistivity at low temperature.

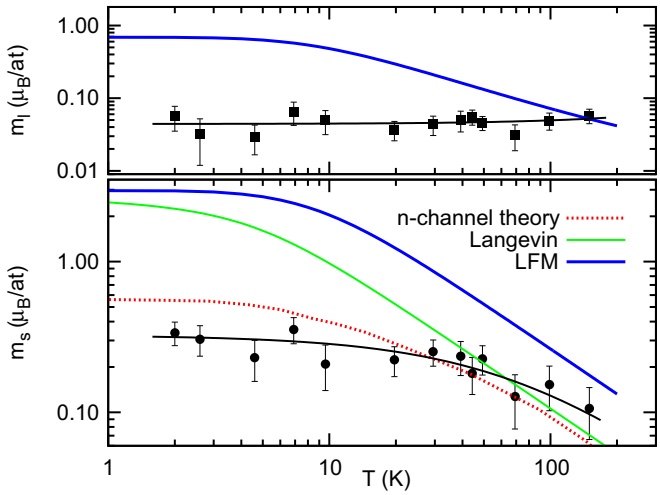

FIG. 3. (a) Spin and (b) orbital magnetic moment per Fe ion as determined from the XMCD sum rules for the 500 ppm sample in a 6.5 T field. The blue lines represent the moments derived from a LFM calculation for the same configuration as in Fig. 2. The Langevin function for a single atom magnetic moment of $m_s = 2.7\mu_B$ in a 6.5 T field is plotted in green. The black lines through the data are guides to the eye. The red dashed line represents n-channel model calculations ($S = 2$ and $n = 4$). This curve was obtained from an interpolation of the data of Ref. [19] to our experimental field of 6.5 T to enable comparison. Since these calculations scale with the Mössbauer data of Steiner *et al.*, the red curve thus also holds for Mössbauer data interpolated to 6.5 T.

from each XMCD spectrum without the need for a normalization to the total absorption intensity. We note that the way the oxide/background is subtracted affects the values of m_s and m_l. The data points result from an average of different sets obtained by slightly changing the subtraction parameters. Roughly half of the error arises from the variability introduced by the subtraction procedure. In Fig. 2 one might distinguish a first regime independent of temperature below about 30–50 K, and a temperature-dependent regime at higher temperatures. The error bars are, however, quite large and a χ^2 test gives indeed a rejection confidence of only 75% for a constant $m_l/m_s(T)$ ratio hypothesis. The LFM calculations, which neglect Kondo correlations, present a weaker temperature dependence compared to the data (see Fig. 2 and Ref. [36]), but it is not possible to unambiguously conclude on the presence of a Kondo effect on the basis of m_l/m_s alone. Hence, it is mandatory to analyze m_s and m_l separately in order to get further information. Note that in the presence of crystal field, the ratio m_l/m_s is not necessarily constant, as it would be for a paramagnetic impurity in spherical symmetry (Fig. 2 and see also Ref. [36]).

In order to extract absolute values of m_s and m_l as a function of temperature, the XMCD signal is normalized to the integral of the isotropic cross section, which is proportional to the number of holes in the $3d$ states, N_h. As the latter was found to be temperature independent, we take $N_h = 3.37 \pm 0.15$ as calculated by DFT for an Fe impurity embedded in a Cu matrix. Our DFT calculations further predict $m_s = 2.72 \pm 0.16\mu_B$ at 0 K for the Fe impurities, a result which is robust against different implementations of the local spin density approximation [36]. Figure 3 shows the temperature dependence of m_s and m_l in a 6.5 T field determined using the XMCD sum rules.

First, we find that at low temperature m_s is much smaller ($\approx$10 times) than the value expected for a paramagnetic Fe atom. This very weak m_s is spectacularly different from what is observed for isolated atoms on surfaces [27,29,30], including Fe on Cu(111) [38], which show magnetic moments of several Bohr magnetons at these temperatures. Such a reduction, on the other hand, is expected for Kondo screening. For comparison, a Langevin function [39] (green line) assuming a spin moment of $2.7\mu_B$ per atom (as obtained by DFT for Fe in Cu) is plotted together with the spin moment obtained by LFM calculations (blue line) for a paramagnetic Fe ion in a cuboctahedral crystal field (Kondo correlations are not included in LFM calculations). Although several crystal field models were tested, none reproduces the experimental behavior of m_s [36]. In addition, we observe that m_s exhibits a crossover from a nearly-temperature-independent regime, identified as the Kondo regime, to a paramagnetic behavior for $T \geqslant T_K$. A χ^2 on $m_s(T)$ yields a rejection confidence of 99% for a constant m_s hypothesis. Although our values for m_s are smaller, this behavior is qualitatively similar to the evolution of the Fe magnetization as determined by Mössbauer spectroscopy [17]. The red dashed curve in Fig. 3 represents n-channel model calculations [19], describing the evolution of the impurity magnetization as a function of temperature in a given magnetic field (see the caption for details) and which also reproduce the Mössbauer data of Steiner *et al.* on dilute Cu:Fe alloys [17].

The 2500 ppm sample yields both a similar temperature evolution and spin moment per isolated Fe atom. The analysis is, however, more complicated in this case, since it requires removal of a paramagnetic Fe pair contribution [36].

The temperature dependence of the orbital moment is in strong contrast with that of the spin moment. Our data reveal a finite m_l value of $(0.04 \pm 0.01)\mu_B$ per atom, which is almost constant with temperature (a χ^2 test indicates that only the constant hypothesis must be retained) and much smaller than the value of $(0.66 \pm 0.04)\mu_B$ reported for Fe impurities on a Cu(111) surface at low temperature [38]. Although a nearly quenched m_l relative to the free-atom value is expected based on the cubic crystal field symmetry and the strong Fe-Cu hybridization [28], such a weak temperature dependence is unexpected. An explanation for this behavior requires taking into account both the on-site correlation within the impurity, as in a ionic model, as well as its many-body interactions with the host.

The above results are now compared to those of an ionic model of Fe impurities in Cu [40]. Consistently with DFT and the best fit of $m_s(T)$ in the paramagnetic regime, we assign a spin $S = \frac{3}{2}$ to the Fe impurities, corresponding to a monovalent $Fe^+(3d^7)$ electron configuration, the one also suggested for the ground state of Fe impurities in simple metal hosts [27], for Fe atoms on a Cu(111) surface [38], and by early Mössbauer and NMR experiments [17,40]. According to the Hund's rules, the lowest-energy atomic term is then the ^4F state with total orbital moment $L = 3$. The cubic crystal field at the Fe sites splits this state into a lower orbital singlet ($^4A_{2g}$) and two upper orbital triplets ($^4T_{2g}$,$^4T_{1g}$). When the spin-orbit interaction is included as a perturbation, the mixing of the higher-energy orbitally degenerate states with the $^4A_{2g}$ ground state results in a finite orbital moment, of the order of $(8\lambda/10Dq)\mu_B$ [41]. Taking the spin-orbit constant of the ^4F Fe term $\lambda \approx 15$ meV and $10Dq = 0.25$ eV for the cubic crystal field splitting, as suggested by our LFM calculations and the NMR data [40], one obtains $m_l \approx 0.5\mu_B$, which we may consider as an upper limit of m_l in the absence of *s*-*d* hybridization and Kondo screening effects. Such a perturbative contribution to the orbital moment, however, besides being too large, is also temperature dependent, in contrast with the behavior reported in Fig. 3. LFM calculations, which provide an exact treatment of spin-orbit-induced mixing of the ground state with higher-energy levels, also yield too large values of m_l at low temperature, unless the on-site electron correlation is reduced to an unusually low level (see Fig. S3 in Ref. [36]). On the other hand, there exists also a smaller, temperature-independent contribution to the orbital moment, which arises from the second-order Zeeman effect. This contribution, which has been discussed but is yet to be quantified in the interpretation of early Mössbauer and NMR studies [17,18], is of the order of $2\mu_B B/10Dq$, where B is the applied magnetic field [40]. In our case, this term may account for about one tenth of the experimental m_l, and is thus too small to provide a satisfactory explanation for the weak temperature dependence of the Fe orbital moment.

This analysis, together with the results of our LFM calculations, indicates that the finite and nearly-temperature-independent m_l cannot be associated with single-ion properties, as determined by the interplay of crystal field, spin-orbit coupling, and Zeeman interactions only. A correct description must consider, for both m_s and m_l, the Kondo effect resulting from the *d*-*d* correlation effects and the hybridization between the *d* orbitals of the impurity and conduction electrons [7,8,42]. Following this hypothesis, our results suggest that Kondo screening of the Fe orbital moment starts to occur at a much higher temperature than for the spin moment, beyond the range probed in the present study.

In conclusion, the XMCD measurements of dilute Cu:Fe alloys reported in this Rapid Communication provide a separate determination of the spin and orbital moments of a Kondo system above and below T_K. The crossover from the free-atom-like paramagnetic regime to the Kondo-screened regime is clearly identified for the spin magnetic moment, which shows Curie-Weiss behavior for $T > T_K$ and saturates at $m_s \approx 0.35\mu_B$ for $T < T_K$ in a magnetic field of 6.5 T, a value much smaller than the "bare" Fe spin magnetic moment of $2.7\mu_B$ calculated by DFT. In contrast with the spin moment, we find the orbital magnetic moment to be nearly temperature independent, remaining close to $m_l = 0.04 \pm 0.01\mu_B$ between 2 and 150 K. In order to understand theoretically such a behavior, and to investigate a possible spin and orbital decoupling, it would be necessary to solve the multiorbital Kondo problem by taking into account not only the Hund's rule coupling and the crystal field effect but also the spin-orbit coupling, which is a very challenging problem.

We are grateful to B. Muller from IPCMS and the SIM beamline staff at Swiss Light Source for their help in setting up the measurements. We would also like to thank N. Lorente, J. Merino, and T. O. Wehling for fruitful discussions. Financial support from CNRS PICS program, Contract No. 5275, the SNSF (Grant No. 200021-153404), as well as computational time from the IDRIS-GENCI (Project No. i2014092291) is acknowledged.

[1] J. Kondo, Rep. Prog. Theor. Phys. **32**, 37 (1964).
[2] P. W. Anderson, Phys. Rev. **124**, 41 (1961).
[3] A. C. Hewson, *The Kondo Problem to Heavy Fermions*, edited by D. Edwards and D. Melville, Cambridge Studies in Magnetism (Cambridge University Press, Cambridge, UK, 1997).
[4] J. R. Schrieffer and P. A. Wolff, Phys. Rev. **149**, 491 (1966).
[5] Ph. Nozières, J. Low Temp. Phys. **17**, 31 (1974).
[6] K. Wilson, Rev. Mod. Phys. **47**, 773 (1975).
[7] L. Dworin and A. Narath, Phys. Rev. Lett. **25**, 1287 (1970).
[8] Ph. Nozières and A. Blandin, J. Phys. (France) **41**, 193 (1980).
[9] T. A. Costi, L. Bergqvist, A. Weichselbaum, J. von Delft, T. Micklitz, A. Rosch, P. Mavropoulos, P. H. Dederichs, F. Mallet, L. Saminadayar, and C. Bäuerle, Phys. Rev. Lett. **102**, 056802 (2009).
[10] B. Gu, J.-Y. Gan, N. Bulut, G.-Y. Guo, N. Nagaosa, and S. Maekawa, J. Phys.: Conf. Ser. **200**, 062007 (2010).
[11] C. Carbone, M. Veronese, P. Moras, S. Gardonio, C. Grazioli, P. H. Zhou, O. Rader, A. Varykhalov, C. Krull, T. Balashov, A. Mugarza, P. Gambardella, S. Lebègue, O. Eriksson, M. I. Katsnelson, and A. I. Lichtenstein, Phys. Rev. Lett. **104**, 117601 (2010).

[12] R. Korytár and N. Lorente, J. Phys.: Condens. Matter **23**, 355009 (2011).
[13] B. Surer, M. Troyer, Ph. Werner, T. O. Wehling, A. M. Läuchli, A. Wilhelm, and A. I. Lichtenstein, Phys. Rev. B **85**, 085114 (2012)
[14] P. D. Sacramento and P. Schlottmann, J. Phys.: Condens. Matter **3**, 9687 (1991).
[15] A. M. Tsvelick and P. B. Wiegmann, Z. Phys. B **54**, 201 (1984).
[16] R. Tournier and A. Blandin, Phys. Rev. Lett. **24**, 397 (1970).
[17] P. Steiner, S. Hüfner, and W. V. Zdrojewski, Phys. Rev. B **10**, 4704 (1974).
[18] H. Alloul, Physica B **86-88**, 449 (1977).
[19] P. D. Sacramento and P. Schlottmann, Solid State Commun. **73**, 747 (1990).
[20] A. Narath, Phys. Rev. B **13**, 3724 (1976).
[21] J.-T. Li, W.-D. Schneider, R. Berndt, and B. Delley, Phys. Rev. Lett. **80**, 2893 (1998).
[22] V. Madhavan, W. Chen, T. Jamneala, M. F. Crommie, and N. S. Wingreen, Science **280**, 567 (1998).
[23] M. Ternes, A. J. Heinrich, and W.-D. Schneider, J. Phys.: Condens. Matter **21**, 053001 (2009).
[24] H. Prüser, M. Wenderoth, P. E. Dargel, A. Weismann, R. Peters, T. Pruschke, and R. G. Ulbrich, Nat. Phys. **7**, 203 (2011).
[25] B. T. Thole, P. Carra, F. Sette, and G. van der Laan, Phys. Rev. Lett. **68**, 1943 (1992).
[26] P. Carra, B. T. Thole, M. Altarelli, and X. Wang, Phys. Rev. Lett. **70**, 694 (1993).
[27] P. Gambardella, S. S. Dhesi, S. Gardonio, C. Grazioli, P. Ohresser, and C. Carbone, Phys. Rev. Lett. **88**, 047202 (2002).
[28] W. D. Brewer, A. Scherz, C. Sorg, H. Wende, K. Baberschke, P. Bencok, and S. Frota-Pessôa, Phys. Rev. Lett. **93**, 077205 (2004).
[29] P. Ohresser, H. Bulou, S. S. Dhesi, C. Boeglin, B. Lazarovits, E. Gaudry, I. Chado, J. Faerber, and F. Scheurer, Phys. Rev. Lett. **95**, 195901 (2005).
[30] P. Gambardella and H. Brune, Surf. Sci. **603**, 1812 (2009).
[31] J. P. Franck, F. D. Manchester, and D. L. Martin, Proc. R. Soc. London, Ser. A **263**, 494 (1961).
[32] J. L. Tholence and R. Tournier, Phys. Rev. Lett. **25**, 867 (1970)
[33] F. B. Huck, Wm. R. Savage, and J. W. Schweizer, Phys. Rev. B **8**, 5213 (1973).
[34] M. A. Blachly and N. Giordano, Phys. Rev. B **51**, 12537 (1995); **49**, 6788 (1994).
[35] J. Krempaski, U. Flechsig, T. Korhonen, D. Zimoch, Ch. Quitmann, and F. Nolting, in *SRI 2009, 10th International Conference on Radiation Instrumentation*, edited by R. Garrett, I. Gentle, K. Nugent, and S. Wilkins, AIP Conf. Proc. Vol. 1234 (AIP, Melville, NY, 2010), p. 705.
[36] See Supplemental Material at http://link.aps.org/supplemental/10.1103/PhysRevB.95.041108 for details on the application of XMCD sumrules, for the oxide-correction of the XMCD spectra, for LFM and DFT calculations, and for results on the 2500 ppm bulk sample.
[37] J. Stöhr and H. König, Phys. Rev. Lett. **75**, 3748 (1995).
[38] G. E. Pacchioni, L. Gragnaniello, F. Donati, M. Pivetta, G. Autès, O. V. Yazyev, S. Rusponi, and H. Brune, Phys. Rev. B **91**, 235426 (2015).
[39] To describe the Fe impurity paramagnetism in the Cu host, we opted for a Langevin function rather than a Brillouin function since the spin of Fe given by DFT calculations is not an integer or half integer. Anyway, both functions yield approximately similar shapes, and the same value at saturation.
[40] D. C. Abbas, T. J. Aton, and C. P. Slichter, Phys. Rev. B **25**, 1474 (1982).
[41] B. N. Figgis and M. A. Hitchman, *Ligand Field Theory and Its Applications* (Wiley-VCH, Weinheim, 2000).
[42] L. L. Hirst, Z. Phys. **244**, 230 (1971).